

# Excitonic Funneling in Extended Dendrimers with Non-Linear and Random Potentials

Subhadip Raychaudhuri<sup>(1)</sup>, Yonathan Shapir<sup>(1)</sup>, Vladimir Chernyak<sup>(2)</sup>, and Shaul Mukamel<sup>(2)</sup>

<sup>(1)</sup>*Department of Physics and Astronomy, University of Rochester, Rochester, NY 14627*

<sup>(2)</sup>*Department of Chemistry, University of Rochester, Rochester, NY 14627*

(November 19, 2018)

The mean first passage time (MFPT) for photoexcitations diffusion in a funneling potential of artificial tree-like light-harvesting antennae (phenylacetylene dendrimers with generation-dependent segment lengths) is computed. Effects of the non-linearity of the realistic funneling potential and slow random solvent fluctuations considerably slow down the center-bound diffusion beyond a temperature-dependent optimal size. Diffusion on a disordered Cayley tree with a linear potential is investigated analytically. At low temperatures we predict a phase in which the MFPT is dominated by a few paths.

Dendrimers constitute a new class of nanomaterials with unusual tree-like geometry and interesting chemical, transport, and optical properties [1–5]. Two families of Phenylacetylene dendrimers have received considerable recent attention. In the compact family, the length of the linear segments is fixed, whereas in the extended family it increases towards the center creating an energy funnel in that direction (Fig. 1). This latter family may, therefore, serve as artificial light-harvesting antennas, as has been demonstrated experimentally [6]. It has been conjectured by Kopelman *et. al.*, based on optical absorption spectra [1], that electronic excitations in these dendrimers are localized on the linear segments. This has been confirmed in theoretical studies which showed that the relative motion of photogenerated electron-hole pairs is confined to the various segments and energy-transfer may then be described by the Frenkel exciton model. The time it takes for an excitation that starts at the periphery to reach the center, and its dependence on the molecular size (number of generations  $g$ ) and the funneling force, were calculated. The latter results from the interplay of entropic (or geometric, *i.e.* the branching ratio  $c = 2$ ) and energetic factors [7].

These pioneering studies, however, assumed the funneling force to be constant since the energy  $\epsilon(n)$  varied linearly with  $n$ . ( $n=1,2,\dots,g$  is the generation number, at which the segment length is  $l = g - n + 1$  monomers. See Fig. 1.) In addition,  $\epsilon(n)$  were assumed to be fixed. In reality, interactions with other degrees of freedom (solvent and intramolecular vibrations), induce fluctuations in  $\epsilon(n)$  which may span many different timescales. Here we consider slow (quenched) fluctuations compared with the exciton trapping times which are typically in the picosecond range [6,8]. Nonlinear [9] and single molecule [10] spectroscopy in liquids, glasses and proteins typically show nanosecond to millisecond bath motions responsible for spectral diffusion. Slow vibrational motions that can be treated as static disorder dominate the photoinduced energy transfer dynamics of photosynthetic antenna complexes [11]. Fast (annealed) fluctuations do not change the behavior qualitatively. In addition, we explore different degrees of correlations among the various energy fluctuations. In the absence of correlations, we obtain the standard diagonal disorder (random energy) model. If the energy differences of nearby segments are coupled to independent baths, we obtain a random force model. Other types of correlations are possible as well. In a recent paper Bar-Haim and Klafter [7] extended their studies to a special kind of disorder with unique correlations between the hopping rates. They also looked at the effect of including a single impurity.

In the present Letter, we address two crucial properties of the funneling potential of dendrimers: (*i*) The nonlinear dependence of the exciton energy on  $n$  is taken from the electronic structure calculations of Tretiak, Chernyak, and Mukamel [12]. (*ii*) The effects of general and realistic types of quenched disorder are investigated. Our study has direct implications on the design of the dendrimers with improved light-harvesting efficiency. We find that the nonlinear potential drastically reduces this efficiency for dendrimers larger than a polymer-specific optimal size (which is found to be in the range of 7-9 generations at room temperature). At the same time the effect of disorder in slowing down the excitonic migration towards the trap, is much more severe for dendrimers larger than this optimal size. Thus, on both counts, efforts to make the dendrimers larger than this size will provide only a modest pay-off in the number of excitons reaching the active center (even though the total photon adsorbance will increase [1]).

Our results differ drastically from the ones found for a linear potential. However, they can be qualitatively understood in the context of the different regimes of diffusion in such a potential. Therefore, we first study the effect of disorder on the diffusion in a linear potential. Interestingly, we find a *dynamic* transition into a highly disordered phase akin to the *equilibrium* replica symmetry breaking found in other random statistical models [13].

The theoretical investigations focused on the mean first passage time (MFPT), which provides an adequate measure for the efficiency of the trapping. Another quantity of interest is the mean residence time (MRT), the average time

spent on a site of the tree (*i.e.*, on a segment of the dendrimer). The starting point for the analysis are coupled master equations for the probability  $p(i, t)$  of the exciton to reside at time  $t$  on the  $i$ th segment. If the potential only depends on the generation  $n$ , the problem reduces to an effectively one-dimensional one for  $p(n, t)$ , which obeys the equations:  $\dot{p}_n(t) = T_{n+1}p_{n+1}(t) + R_{n-1}p_{n-1}(t) - (T_n + R_n)p_n(t)$ , where  $T$  ( $R$ ) are the rate constants for transfer towards the periphery (center) and absorbing (reflecting) boundary condition are used at  $n = 0$  ( $n = g$ ).

We define the detailed-balance ratio  $\xi(n) = R_n/T_{n+1} = c \exp\{-\beta[\epsilon(n+1) - \epsilon(n)]\}$ . For simplicity we assume  $T_n = 1$  for all  $n$ . For excitation starting at the periphery, the MRT on the  $n$ th site is given by [7]:  $t_n = (\sum_{m=1}^{n-1} \prod_{j=n-m}^{n-1} \xi_j) + 1$ . The MFPT is given by the sum over the  $t_n$ 's:  $\tau_g = \sum_{n=1}^g t_n$ . For a linear potential  $\xi(n) = \xi_0 = c \exp(-\beta f)$ , where  $f$  is the  $n$ -independent potential-difference and  $\beta$  is the inverse temperature (room temperature is assigned unless specified otherwise), one finds [7]:

$$\tau_g = \xi_0 \frac{\xi_0^g - 1}{(\xi_0 - 1)^2} - \frac{g}{\xi_0 - 1}, \quad \xi_0 \neq 1. \quad (1)$$

Eq. (1) shows three regimes for the scaling of  $\tau_g$  with  $g$ : For  $\xi_0 > 1$ :  $\tau_g \sim \exp(g \ln \xi_0)$  (exponential regime) for  $\xi_0 < 1$ :  $\tau_g \sim g$  (linear regime) and at the transition,  $\xi_0 = 1$  (for a critical force  $f_c = \ln c/\beta$ ), the behavior is purely diffusive (quadratic):  $\tau_g \sim g^2$  [7].

### Nonlinear TDHF potential.

The exciton energies of linear segments of acetylene units have been calculated in [12] using the time-dependent Hartree Fock (TDHF) technique. These energies can be fitted to the following nonlinear expression [14]:

$$\epsilon(n) = A \left[ 1 + \frac{L}{g - (n - 1)} \right]^{0.5}, \quad (2)$$

with  $A = 2.80 \pm 0.02$  (eV) and  $L = 0.669 \pm 0.034$ .

The MFPT for an exciton generated at the periphery on this potential is depicted in Fig. 2, for different temperatures. Its variation with  $g$  differs substantially from that of a linear potential. Although the MFPT depends linearly on  $g$  for the first few generations, it gradually crosses over (for  $n \geq 7$ ) to an exponential behavior with increasing  $g$ . As the temperature is reduced, this crossover scale increases due to the entropic effect.

The MRT is not a monotonic function of  $n$ . For large  $g$ , at the generations near the periphery ( $g - n \ll g$ ) the funneling force is strong and overcomes the entropic effect of  $c \geq 2$  which ‘‘pushes’’ the exciton outward. Near the center, however, the larger is  $g$ , the weaker is the funneling force and the entropic term dominates. As a result the exciton spends most of its time at some intermediate generation  $n = n^*(g)$  close to where the two effects nearly cancel and the net thermodynamic force is minimal. In Fig.(3), we display the reduced free-energy  $u(n) = \beta\epsilon(n) - n \ln c$ , and the MRT, vs  $n$  for  $g = 14$ . The MRT is maximal at  $n^*(14) = 8$  close to where  $u(n)$  is minimal. As  $g$  increases beyond  $g \approx 9$ , both  $n^*$  (Fig. (3)) and the energy difference  $\Delta u(n^*) = u(1) - u(n^*)$  increase with  $g$ . Hence, the time to reach the center from  $n^*$  grows exponentially with  $g$  (the time to arrive at  $n^*$  is much shorter).

### Random Cayley tree with a linear potential.

We begin the investigation of the effects of disorder by first considering a linear potential. Four models were studied: (i) *Random intergenerational energy* - The same random energy is assigned to all the segments in a given generation. (ii) *Random intergenerational force* - The energy differences between consecutive generations are randomly distributed. (iii) *Random intersegment energy* - All segment energies are random and uncorrelated, and (iv) *Random intersegment force* - All energy differences between neighboring segments are random. The mapping to an effective one-dimensional model applies for the first two models only. We set  $\xi_n = \xi_0 \exp(-\beta\Delta\epsilon_n)$  with  $\Delta\epsilon_n = \epsilon_{n+1} - \epsilon_n$ . The behavior for each of the models is as follows:

(i) *Random intergenerational energy*: This model whereby  $\epsilon(n)$  have an identical distribution  $P(\epsilon)$  (with  $\langle \epsilon_n \rangle = 0$ ,  $\langle \rangle$  denotes average over the disorder), has been investigated [15] with the following implications to our system: We define  $\eta \equiv \exp(-\beta\epsilon)$  and assume finite values for  $\langle \eta^{\pm 1} \rangle$  and  $\langle \eta^{\pm 2} \rangle$ . The average MFPT (up to  $g$ -independent constants) is given by:  $\langle \tau(g) \rangle = \langle \eta \rangle \langle \eta^{-1} \rangle \tau_0(g)$  with the three regimes of behavior (linear, quadratic and exponential) depending on  $\xi_0$  being  $<$ ,  $=$ , or  $>$  1. For example, for a Gaussian distribution  $P_G(\epsilon) = (1/\sqrt{2\pi\lambda}) \exp\{-\epsilon^2/2\lambda^2\}$ ,  $\langle \tau(g) \rangle$  is enhanced by a  $\exp(\beta^2\lambda^2)$  factor compared with  $\tau_0(g)$ . The disorder then slows down the funneling, but leaves the  $g$ -dependence unchanged. Another important effect of disorder is to induce fluctuations in the MFPT  $\langle \Delta\tau^2 \rangle = \langle (\tau - \langle \tau \rangle)^2 \rangle$ . The relative fluctuations  $\delta\tau/\tau = \langle \Delta\tau^2 \rangle^{1/2}/\langle \tau \rangle$  scale as  $\sim 1/\sqrt{g}$ , in the linear regime and at the quadratic point, and is a  $g$ -independent constant in the exponential regime.

(ii) *Random intergenerational force*: This model assumes  $\Delta\epsilon_n$  to be independently distributed according to a distribution  $P(\Delta\epsilon)$  and is reviewed in [16]. Proceeding along similar lines, we find the following regimes: (a)  $\langle \xi \rangle < 1$ :

$\langle \tau(g) \rangle$  is linear in  $g$ .  $\langle \tau^2(g) \rangle \sim g^2$  as long as  $\langle \xi^2 \rangle < 1$ , while if  $\langle \xi^2 \rangle > 1$ ,  $\langle \tau^2(g) \rangle$  grows exponentially with  $g$  as the typical behavior begins to differ from the average. (b)  $\langle \xi \rangle > 1$ , but  $\langle \ln \xi \rangle < 0$ :  $\langle \tau(g) \rangle$  is exponential in  $g$  and so are the relative fluctuation  $\delta\tau/\tau$ . The average is determined by rare configurations, while the more representative  $\tau_{typ} = \exp \langle \log \tau(g) \rangle$  behaves as  $g^\alpha$  with  $\alpha = \langle \delta(\ln \xi)^2 \rangle / 2 \langle \ln \xi \rangle [= \beta^2 \lambda^2 / 2 (\ln \xi_0)]$  for  $P_G(\Delta\epsilon)$ . (c)  $\langle \ln \xi \rangle = 0$  [17]:  $\langle \tau(g) \rangle$  is exponential in  $g$  while  $\tau_{typ}(g)$  is exponential in  $\sqrt{g}$  [18]. (d)  $\langle \ln \xi \rangle > 0$  both  $\langle \tau(g) \rangle$  and  $\tau_{typ}(g)$  diverge exponentially with  $g$ .

(iii) *Random intersegment energy*: We extended the calculations of model (i) to the fully random-energy tree with almost identical results. The main difference is that, for intersegment disorder, additional fluctuations in the MFPT arise from distinct initial sites at the periphery. In all regimes their  $g$  dependence is identical to that due to dendrimer-to-dendrimer fluctuations.  $\delta\tau/\tau$  (from both effects) saturates, at large disorder, to a value smaller than the corresponding one in model (i).

(iv) *Random intersegment force*: The techniques applied in model (ii) may not be simply generalized to the fully random-force tree. Using the *replica trick*, we have found a one-step replica symmetry breaking (1RSB) transition [13] between a weakly disordered (or high-temperature) phase in which all paths contribute to  $\tau(g)$  and a highly-disordered (low-temperature) phase in which only a small number of them do. Mathematically, the transition is determined by the parameter  $0 < m \leq 1$  for which the value of  $[\xi_0 \langle \exp(-\beta m \Delta\epsilon_n) \rangle]^{1/m}$  is minimal.  $m = 1$  in the high-temperature phase, limited to  $\beta\lambda < \sqrt{2 \ln c}$  for  $P_G(\Delta\epsilon)$ , for which  $f_c = \ln c / \beta + \beta\lambda^2 / 2$  in this phase. In the low-temperature “glassy” phase  $m = \beta\lambda / \sqrt{2 \ln c} < 1$ , and the critical force  $f_c = \lambda\sqrt{2 \ln c}$  is *temperature-independent*.

### **Nonlinear TDHF potential with quenched random energies.**

We have carried Monte Carlo simulations of the effect of disorder on the MFPT for the TDHF nonlinear potential. Disorder is introduced by allowing the energies  $\epsilon(n)$  to fluctuate uniformly in the range of  $\pm 2\%$  around their pure TDHF value  $\epsilon_0(n)$  (Eq. (2)) [19].

Fig.4 shows the disorder-averaged (over  $10^4$  realizations) MFPT for both intergenerational and intersegment types of disorder [such as models (i) and (iii)], compared with the pure TDHF potential. The effect of disorder to increase  $\langle \tau(g) \rangle$ , is clearly more pronounced in the exponential regime. The plots of  $\langle \tau(g) \rangle$  for intergenerational and intersegment disorder are indistinguishable. Their relative fluctuations, however, do differ for large  $g$ .  $\delta\tau/\tau$  saturates to two different values (inset of Fig.4) that of the intergeneration disorder being larger. All these results may be understood from our analytical analysis of models (i) and (iii) above.

In summary, we have shown that the realistic non-linear potential induces an effective funneling only for molecules smaller than some optimal size. For larger dendrimers the free energy has its minima at  $n^*(g)$  where the excitons spend the largest amount of time. For a large production rate of long-lived photoexcitations, we expect the excitons to accumulate at  $n^*(g)$ , at which case the single-exciton picture is not applicable and the exciton-exciton interactions and annihilation processes need to be accounted for [8]. Disorder slows the excitation diffusion towards the center. This effect is always stronger if the MFPT of the corresponding pure system is in the exponential regime. Hence, in order to minimize this slowing down due to randomness, the dendrimers have to be smaller than the same optimal size. Finally, we have uncovered a new effect of increasing force-randomness (or lowering temperature) on the dynamics: the MFPT is dominated by a few paths along the tree. It should be pointed out that not only the average MFPT but the complete distribution of  $\tau(g)$  is readily available experimentally from the time resolved fluorescence profile of the antenna or an acceptor at the center. It will be interesting to explore experimentally this distribution and especially its dependence on the number of generations, and the temperature.

## **ACKNOWLEDGMENTS**

We wish to thank Dr. Sergei Tretiak for useful discussions. The NSF support is gratefully acknowledged.

- 
- [1] R. Kopelman, M. Shortreed, Z. Shi, W. Tan, Z. Xu, J. Moore, A. Bar-haim and J. Klafter, *Phys. Rev. Let.* **78**, 1239 (1997).  
[2] D. A. Tomalia, A. M. Naylor, and W. A. Goddard, *Chem. Int. Ed. Engl.*, **29**, 138 (1990).  
[3] D. -L. Jiang and T. Aida, *Nature (London)*, **388**, 454 (1997).  
[4] V. Blazani, S. Campagna, G. Denti, A. Juris, S. Serroni, and M. Venturi, *Acc. Chem. Res.*, **31**, 26 (1998).

- [5] J. Frechet, *Science*, **263**, 1710 (1994).
- [6] C. Devadoss, P. Bharathi, and J. S. Moore, *J. Am. Chem. Sec.*, **118**, 9635 (1996); M. Shortreed, Z-Y. Shi, and R. Kopelman, *Mole. Cryst. Liq. Cryst.*, **28**, 95 (1996); M. R. Shortreed, S. F. Swallen, Z-Y. Shi, W. Tan, Z. Xec, C. Devadoss, J. S. Moore, and R. Kopelman, *J. Phys. Chem. B.*, **101**, 6318 (1997).
- [7] A. Bar-Haim, J. Klafter, and R. Kopelman, *J. Am. Chem. Soc.* **119**, 6197 (1997); A. Bar-Haim and J. Klafter, *J. Phys. Chem. B* **102**, 1662 (1998); A. Bar-Haim and J. Klafter, *J. of Luminescence* **76-77**, 197 (1998); A. Bar-Haim and J. Klafter, *J. Chem. Phys.* **109**, 5187 (1998).
- [8] M. Pope and C. E. Swenberg, *Electronic Processes in Organic Crystals.*, Second Edition, Oxford University Press, Oxford, New York, 1999.
- [9] C. W. Rella, A. Kwok, K. D. Rector, J. R. Hill, H. A. Schwettmann, D. D. Dlott, and M. D. Fayer, *Phys. Rev. Lett.*, **77**, 1648 (1996).
- [10] H. P. Lu and X. S. Xie, *Nature*, **385**, 143 (1997).
- [11] T. Pullerits, V. Sundstrom, R. van Grondelle, *J. Phys. Chem. B.*, **103**, 2327 (1999).
- [12] S. Tretiak, V. Chernyak and S. Mukamel, *J. Phys. Chem. B* **102**, 3310 (1998).
- [13] B. Derrida, *Phys. Rev. Lett.* **45**, 79 (1980); B. Derrida and H. Spohn, *J. Stat. Phys.* **51**, 817 (1988); Y.Y. Goldschmidt, *J. Phys.* **A31**, 9157 (1998).
- [14] S. Tretiak, V. Chernyak and S. Mukamel, *Phys. Rev. Lett.* **77**, 4656 (1996).
- [15] K. P. N. Murthy and K. W. Kehr, *Phys. Rev. A* **40**, 2082 (1989).
- [16] J. P. Bouchaud and A. Georges, *Phys. Reports* **195**, 127 (1990).
- [17] Ya. G. Sinai, *Russ. Math. Survey* **25**, 137 (1970).
- [18] S. H. Noskowitz and I. Goldhirsch, *Phys. Rev. Let.* **61**, 500 (1988).
- [19] For a Gaussian distribution with mean and standard deviation equal to that of the constant distribution, we found  $\tau(g)$  to diverge faster with  $g$ , due to the dominant effect of the largest energies.

FIG. 1. Extended Phenylacetylene Dendrimer with  $g = 4$  generations.

FIG. 2. The MFPT *vs*  $g$  for the TDHF nonlinear potential at different temperatures (Inset: same for  $g < 5$  magnified).

FIG. 3. Left: The MRT *vs*  $n$  for the TDHF potential, for different values of  $g$ . Right: The reduced free-energy  $u(n)$  for  $g = 14$ .

FIG. 4. The MFPT for the TDHF potential with both types of random energy (indiscernible from each other) compared to that of the pure system (*Inset*: Their relative *rms* variations *vs*  $g$ ).

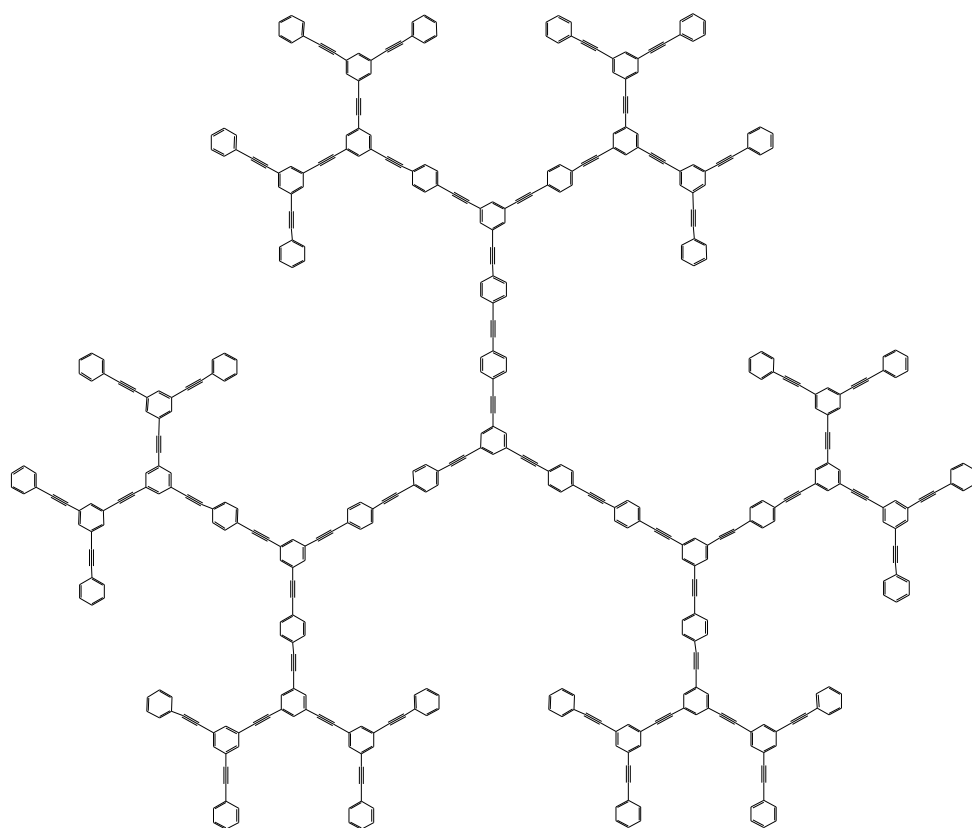


Figure 1

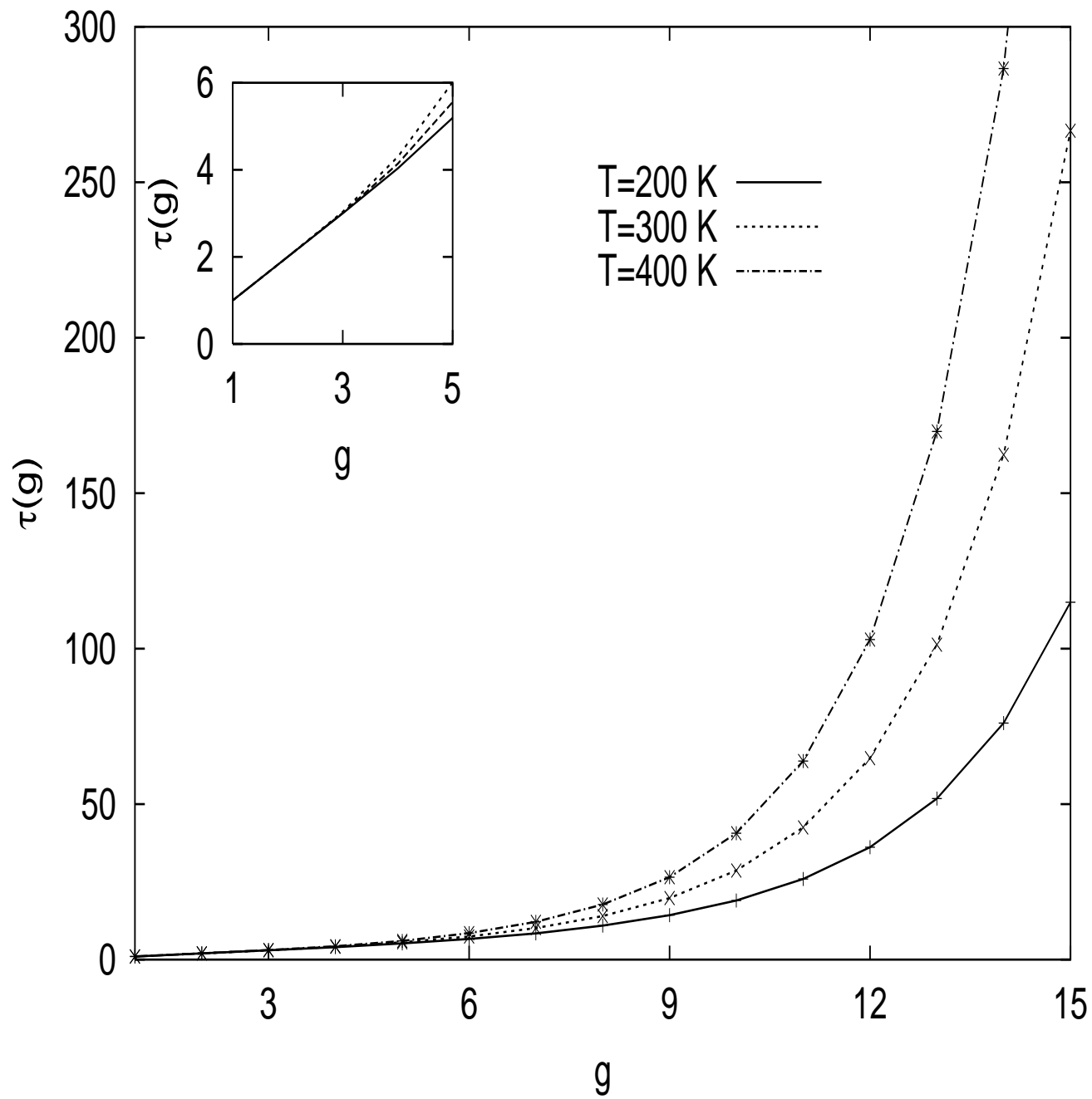


FIG. 2

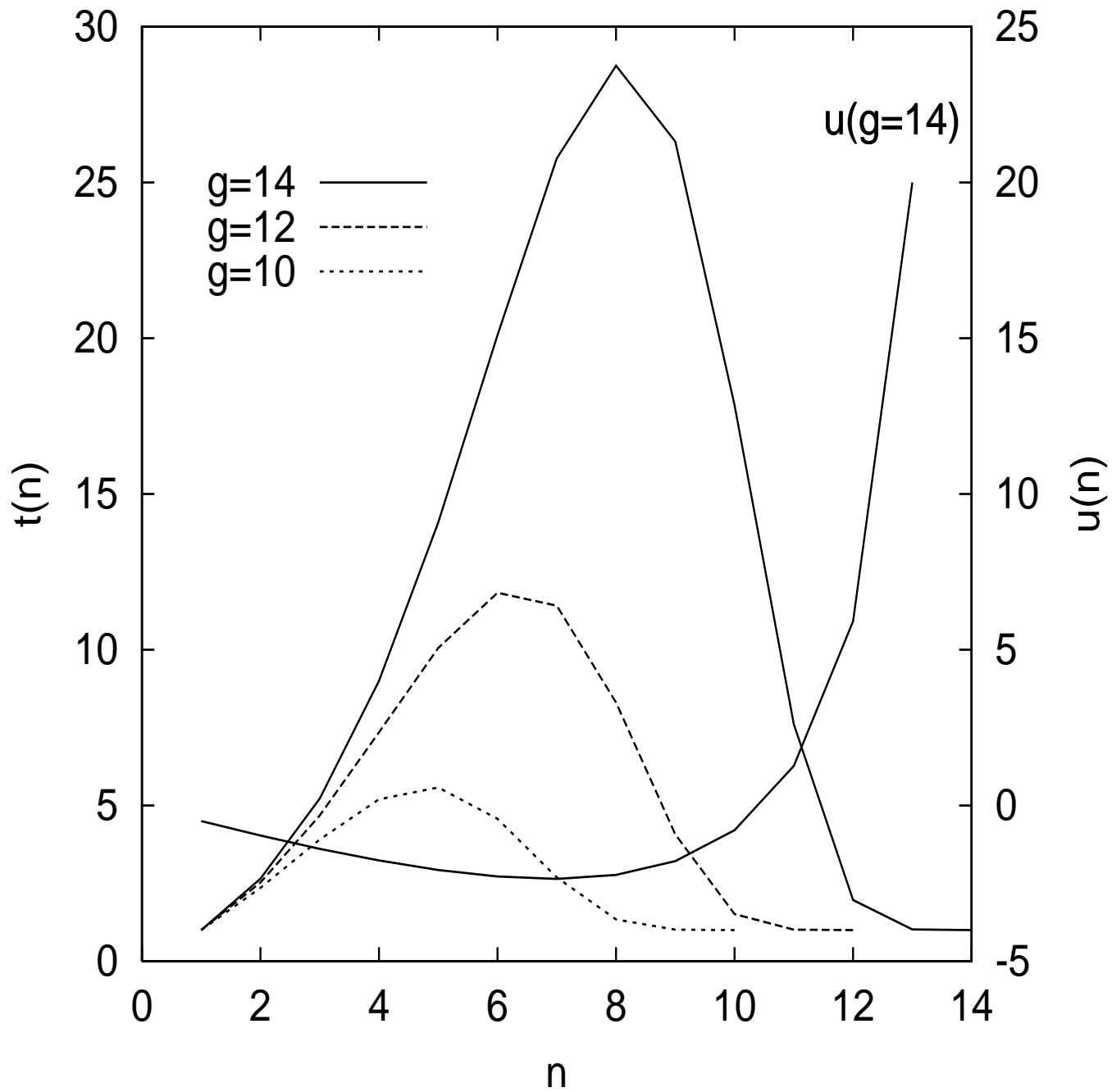


FIG. 3

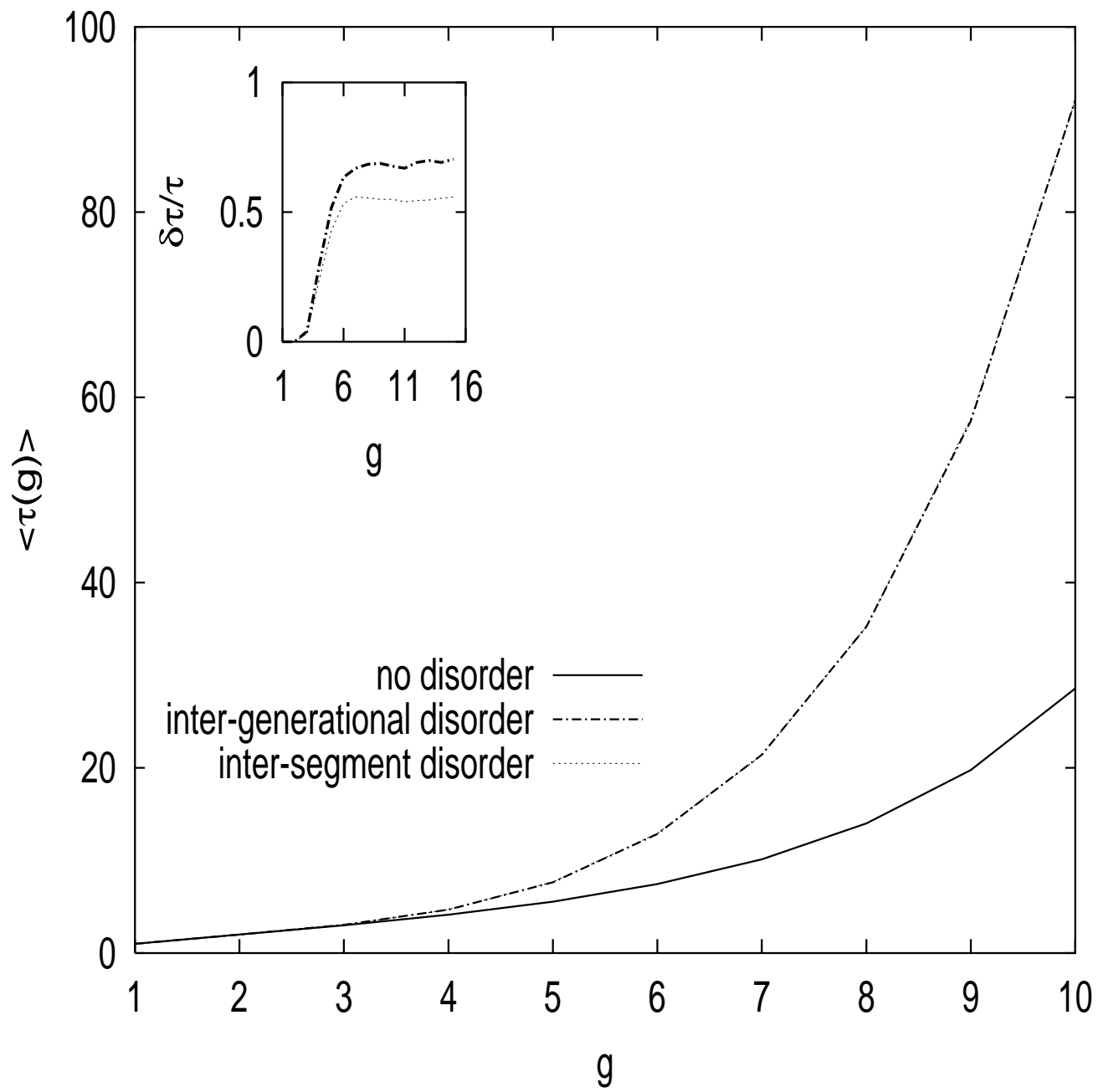


FIG. 4